A Steel Database for Modeling Post-Buckling Behavior And Fracture of Concentrically Braced Frames Under Earthquakes

D.G. Lignos, E. Karamanci & G. Martin
McGill University, Montreal, Canada

SUMMARY
Performance-Based Earthquake Engineering necessitates the development of simulation models that can predict the nonlinear behavior of structural components as part of a building subjected to seismic loading. For the reliable seismic assessment of buildings, these models need to be calibrated with large sets of experimental data. This paper discusses the development of a database that includes extensive information from 295 tests of steel braces that have been conducted worldwide. Statistical information of various properties of steel braces that can be used for quantification of modeling uncertainties is summarized. Through extensive calibration of an inelastic cyclic model that is able to simulate fracture of steel braces due to low cycle fatigue, recommendations for modeling the nonlinear behavior of steel braces are also presented. The utilization of the steel brace database is illustrated through a case study of a 2-story steel special concentrically braced frame.

Keywords: steel braces, post-buckling behavior, fracture, component databases, deterioration

1. INTRODUCTION

The seismic performance assessment of buildings subjected to earthquakes from the onset of damage through collapse necessitates the use of reliable hysteretic models that describe the cyclic behavior of various structural components. In the context of Performance-Based Earthquake Engineering (PBEE), specific damage states are associated with large deformations in which strength and stiffness deterioration of structural components in combination with P-Delta effects trigger dynamic collapse of a building. A key issue to trace the collapse capacity of steel braced frames subjected to earthquakes is to simulate the post-buckling behavior and fracture of the steel braces. To date, a number of models with varying complexity have been proposed for this purpose (e.g., Ikeda et al. 1984, Jin and El-Tawil 2003, Uriz and Mahin 2008, Krishnan 2010, Huang and Mahin 2010). The main challenge to reliably predict the strength and stiffness deterioration of steel braces and subsequently the dynamic behavior of steel braced frames is to accurately represent the input model parameters that control global/local instabilities and ultimately fracture. Another challenge is the treatment of modeling uncertainties of steel braces and their effect on the seismic performance of steel frame buildings through collapse.

Therefore, the development of a steel brace database is needed that permits the calibration and further refinement of analytical models that describe the post-bucking behavior and fracture of various types of steel braces that are commonly used in steel construction. This database should provide statistical information of various properties of steel braces for the quantification of the effects of modeling uncertainties on the earthquake response of steel braced frames. The database should include axial load–deformation hysteretic diagrams of steel braces in a digitized format. Lignos and Krawinkler (2011) developed and demonstrated the utilization of a comprehensive database for deterioration modeling of steel beams in support of collapse assessment of steel moment frames subjected to earthquake loading. Regarding steel braces, Tremblay (2002) and Lee and Bruneau (2005) compiled a dataset of 76 and 66 specimens, respectively. However, these datasets were primarily used (1) to assess the expected post-buckling compressive resistance of steel braces at different compression

ductility levels, (2) to quantify the extent of hysteretic energy dissipation achieved by braces in compression and (3) to develop regression equations that estimate the out-of-plane rotation of braces to fracture. None of these datasets includes digitized axial load-displacement hysteresis diagrams, which are critical for calibration of the input parameters of the steel brace hysteretic models. More recently, Hsiao et al. (2012) compiled a dataset of 44 Hollow Square Steel (HSS) sections. Based on this data, they developed a strain-based analytical model in the OpenSees platform (McKenna 1997) that is able to simulate the buckling capacity and post-buckling response of Special Concentrically Braced Frames (SCBFs).

This paper discusses the development of a steel brace database of 295 steel braces subjected to cyclic loading. This database is used to obtain central values and measures of dispersion of critical parameters associated with buckling capacity, post-buckling behavior and fracture due to low cycle fatigue of steel braces. This is done through extensive calibration of an analytical model that simulates these phenomena and is currently implemented in the OpenSees platform. The database also serves for the development of drift-based fragility curves for steel braces that express the probability of being or exceeding three discrete damage states that a steel brace can undergo as part of a steel braced frame during an earthquake. The utilization of the steel brace database is demonstrated with a case study of a 2-story SCBF, which was tested at the University of California at Berkeley.

2. STEEL BRACE DATABASE

The steel brace database is a compilation of data from 20 major experimental programs that were conducted from the early 1970s to date around the world. The data was extracted directly from the experimental reports and was organized in metadata and reported results. The former consists of the brace configuration, geometry, and measured material properties for both the steel brace and the gusset plates (if applicable). Reported results contain direct measurements as reported in the test documentation including the digitized histories of axial force-displacement and lateral load-story drift ratio hysteresis diagrams. Most of the reported results had to be digitized from the actual experimental reports. The digitization process was conducted with a software called Digitizer (Lignos 2008), which was developed in JAVA-programming language. The steel brace sections include: 143 HSS, 51 Pipes, 37 L-, 50 W-, 5 WT-shapes and back-to-back channels. These shapes are fabricated by thirteen different steel grades (see Section 2.1). The test configurations that are considered are shown in Fig. 2.1. The brace effective slenderness ratios (KL/r) in the plane of buckling varied from 22.4 to 200. The slenderness parameter λ defined based on Eqn. 2.1 varied from 0.26 to 3.0. In this equation, K is the effective length factor with respect to the axis of buckling, L is the length of the brace, r is the radius of gyration with respect to the axis of buckling, F_y is the measured material yield stress and E is the modulus of elasticity for steel. The brace length of the specimens L_B (see Fig. 2.1) ranged from 410mm to 6230mm and the tensile yield strength $A_g F_y$ ranged from 50kN to 6430kN.

$$\lambda = \frac{KL}{r}\sqrt{\frac{F_y}{\pi^2 E}} \tag{2.1}$$

Based on the width-to-thickness b/t (local slenderness) ratios of the brace cross sections contained in the database, most of the braces comply with the CSA-S16-9 (2009) requirements for Ductile Braced Frames since they are classified as Class 1 according to the section classification limits per CISC (2010) requirements. Thirty braces are classified as Class 2 based on the same limits. The steel brace classification is slightly different according to the AISC 360-10 (2010) requirements. Therefore, only thirty-three (33) braces are classified as moderate ductility members. The rest are highly ductile members. The majority of the steel braces that were collected in the database developed a plastic hinge at a distance about one half of their full length (center location). Fracture due to low cycle fatigue was initiated at the same location. A number of braces that failed due to weld premature fracture in their connection are also included in the database but they are not part of the evaluation discussed in Sections 2.2 and 2.3.

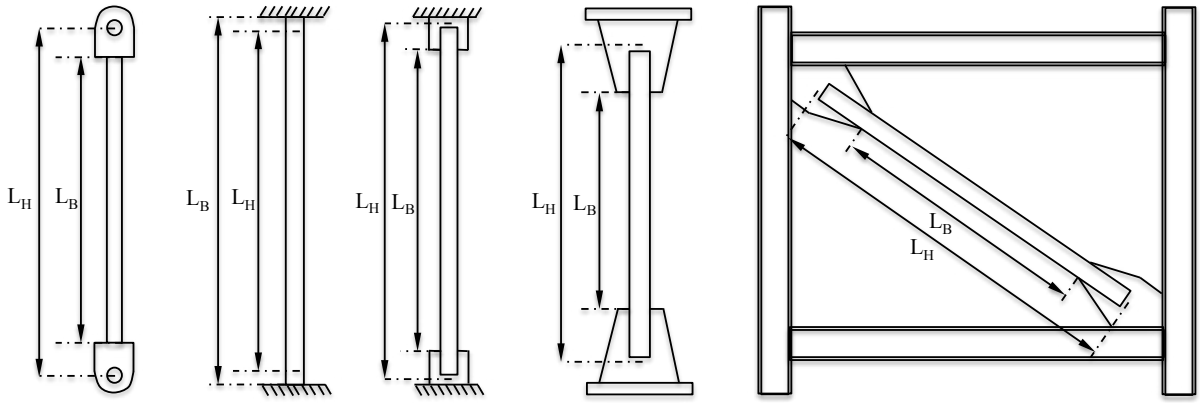

Figure 2.1 Steel brace configurations considered in the steel brace database

2.1. Statistical information on material properties of steel braces

The steel brace database provides an opportunity to compute statistical information of the measured yield and ultimate stresses of various steel grades that are commonly used in steel construction. This information is valuable since it can be used to assess the current expected yield strength of steel braces that is used in the design practice. Furthermore, this information can be used to quantify modeling uncertainties and their effects on the global seismic performance of steel braced frames (Victorsson 2011). Table 2.1 summarizes the main steel grades and shapes together with their nominal yield stress ($F_{y,n}$). In the same table, the average (μ), standard deviation (β) and Coefficient of Variation (COV) of measured-to-nominal yield ratios ($F_{y,m}/F_{y,n}$) is also presented based on counted statistics. These values can be directly compared with recommended R_y values as reported in current design provisions. The observed differences are attributed in part to (1) various shapes and (2) fabrication processes during time and region.

Table 2.1. Statistical information of material properties of steel braces

Steel Grade	Shapes	N	$F_{y,n}$ [*MPa*]	R_y (based on current design provisions)	$F_{y,m}/F_{y,n}$		
					μ	β	COV
ASTM A36/A36M	W, WT, L	23	250	1.5	1.19	0.12	0.10
ASTM A500 Gr. B	HSS, P	52	315	1.4	1.40	0.13	0.09
ASTM A53/A53M	P	12	240	1.6	1.31	0.29	0.22
A992/A992M	W	5	345	1.1	1.15	0.07	0.06
AISI 1020	P	6	295	-	1.13	0.64	0.57
ASTM A500 Gr. C	HSS, P	14	345	1.4	1.16	0.17	0.15
ASTM A501	HSS	3	250	1.4	2.05	0.37	0.18
ASTM A570-Gr. C	HSS	24	230	-	1.21	0.19	0.16
S235JRH	HSS	16	235	-	1.59	0.44	0.28
CSA-G40.21-350W	HSS	53	350	-	1.20	0.11	0.09
SS400 (SS 41)	P, W, L	63	235	-	1.36	0.25	0.19
M1020	L	8	200	-	1.82	0.04	0.02
STK400 (STK 41)	P	9	235	-	1.51	0.03	0.02

2.2. Development of fragility curves for different damage states of steel braces

The steel brace database has been utilized to develop drift-based fragility curves for steel braces to estimate the probability of reaching or exceeding three discrete damage states (DSs). Damage State 1 (DS1) corresponds to global (flexural) buckling of the steel brace. Damage State 2 (DS2) corresponds to local buckling at the center of a steel brace where a plastic hinge forms. The last damage state (DS3) is associated with loss of strength due to fracture at the plastic hinge region. All three damage states are shown in Figs. 2.2a-2.2c (photos from Fell et al. 2009). Since the occurrence of these damage states is not necessarily reported in most of the experimental reports, the associated drift values for each damage state are directly extracted from the hysteretic response of the steel braces

based on the definitions that are shown in Figure 2.2d. Braces that fail in a brittle manner at their ends due to premature fracture as well as damage states associated with yielding of the gusset plates are not considered as part of this investigation. Figures 2.2e to 2.2g show the drift-based cumulative frequency distribution functions for HSS braces for the three damage states that were discussed above. For each damage state, it was found that a lognormal probability distribution provides the best fit. The parameters of the lognormal distributions were found through the method of maximum likelihood (Venables and Ripley 2002). These cumulative distributions are showed in Figs. 2.2e to 2.2g. In order to verify if the cumulative distributions could be assumed as lognormally distributed, a Kolmogorov-Smirnov (K-S) goodness-of-fit test was conducted with a 5% significance level for the individual damage states. The lognormal assumption hypothesis is acceptable for all three damage states as shown in Figs 2.2e-2.2g.

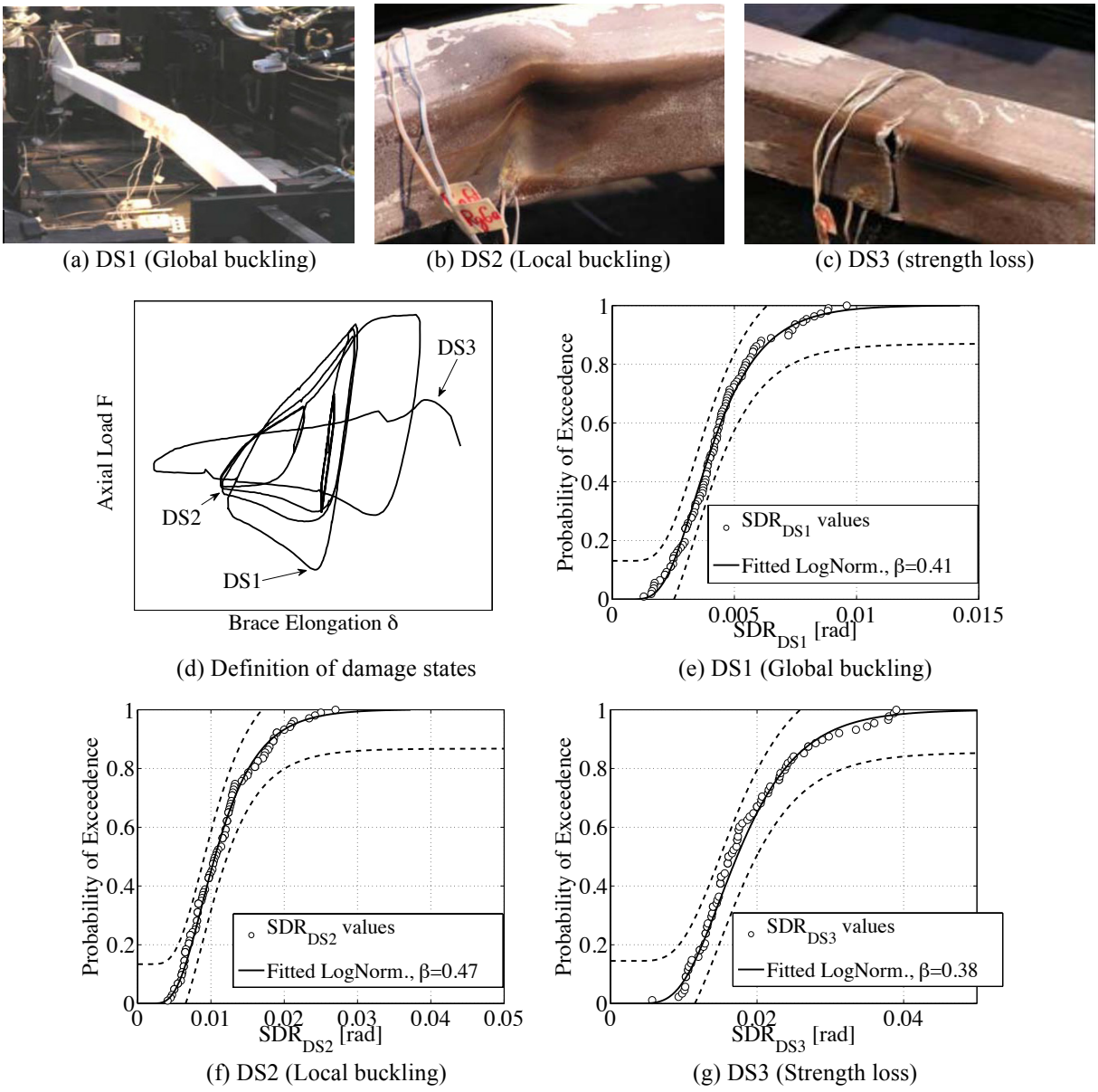

Figure 2.2 Damage states for steel braces; drift-based fragility functions for each damage state (Photos from Fell et al. 2009)

The corresponding parameters of the fitted lognormal distributions are summarized in the same figures. The dispersion values β for DS1, DS2 and DS3 are 0.41, 0.47 and 0.38, respectively. This indicates that if only peak story drift ratios are used to quantify structural damage in steel braced frames, the fragility curves shown in these figures still provide a reliable way to estimate the

likelihood of buckling (global and local) and fracture due to low-cycle fatigue. The authors have also developed fragility curves for other steel shapes (Pipes, W, L) that are commonly used in modern construction of steel braced frames and have formed similar conclusions.

2.3. Modeling of post-buckling behavior and fracture of steel braces

This section provides information regarding the missing aspect of comprehensive numerical modeling of the post-buckling behavior and fracture due to low cycle fatigue of steel braces subjected to cyclic loading. A recently developed numerical model (Uriz and Mahin 2008) that describes the hysteretic behavior of steel braces is extensively calibrated for this purpose with the available experimental data.

2.3.1. Modeling Approach

In order to model the post-buckling behavior of a steel brace, the model proposed by Uriz and Mahin (2008) is utilized in OpenSees. This model is based on a force formulation that was originally proposed by Spacone et al. (1996). With the use of a single element the curvature distribution can be sufficiently represented along the entire brace length. A brace component is divided to at least eight elements (see Fig. 2.3a) based on a sensitivity study that was conducted with a subset of HSS braces. A fiber approach is used to model the cross section of the brace in order to account for the interaction of axial force and bending along the brace. The Menegotto-Pinto (1973) uniaxial material is assigned to each one of the fiber elements (see Fig. 2.3b) in order to simulate the engineering stress-strain behavior of the steel material. The Gauss-Lobatto quadratic rule with two integration points at the element ends is used for the numerical integration within each element. To model global buckling, an initial camber is necessary. For this reason a 0.1% of the brace length was found to be adequate to model this camber. The corotational transformation is used to capture the member geometric effects. It should be pointed out that while local buckling typically occurs at the center of a steel brace, the modeling approach discussed herein does not account for this phenomenon.

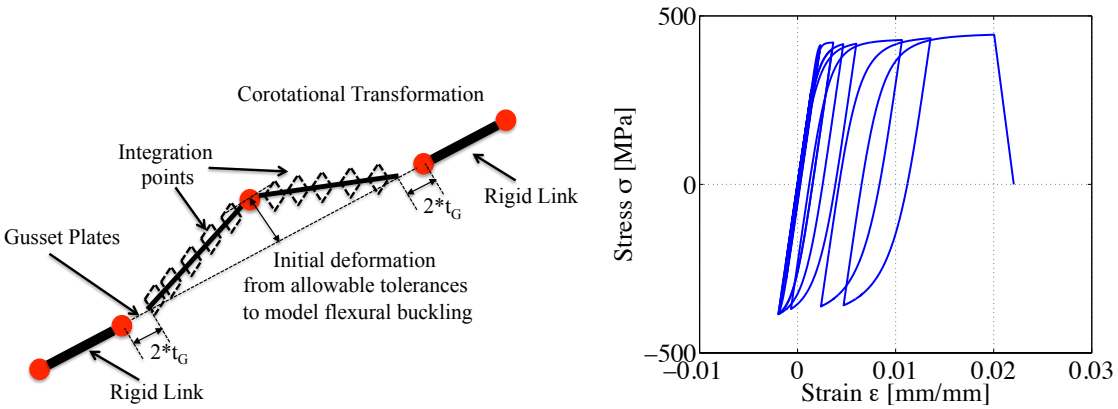

(a) Nonlinear beam-column element (b) Uniaxial stress-strain relationship

Figure 2.3 Numerical model for post-buckling behavior of steel braces subjected to cyclic loading

Fracture due to low-cycle fatigue is also incorporated in the numerical model of the steel brace. This is based on a linear strain accumulation assumption based on a Coffin-Manson relationship (Manson 1965) in the logarithmic domain as described in Eqn. 2.2.

$$\varepsilon_i = \varepsilon_o \left(N_f \right)^m \tag{2.2}$$

In this equation, ε_o is a material parameter that indicates the strain amplitude ε_i at which one complete cycle of a undamaged material will cause fracture. The coefficient m is a material parameter that relates the sensitivity of the total strain amplitude of the material to the number of cycles to fracture N_f. Fracture is initiated according to a rain-flow-counting rule. A fatigue uniaxial material is used for this purpose, which is available in OpenSees. This material wraps around the hysteretic material shown in

Fig. 2.3b and does not influence the stress-strain behavior of the parent material. When fracture is initiated, the stress in the fiber section drops to zero (see Fig. 2.3b). The calibration process of ε_o and m is summarized in the following section.

2.3.2. Calibration Process

The calibration process of the numerical model that is used to trace the steel brace behavior through fracture is based on principles of engineering mechanics and an optimization process that was developed. An interactive interface has been developed in MATLAB to facilitate this effort. The measured material and geometric properties of each brace are directly used as an input into the OpenSees model to define the geometry and uniaxial material model parameters. It was found that a constant strain-hardening ratio of 0.1% may be used for all the calibrations. In order to calibrate the parameters ε_o and m, the Mesh Adaptive Search Algorithm (MADS) is used (Abramson et al. 2009). The objective function H of the constrained optimization problem is the square root of the sum of the squares of the differences between the simulated $F_{simul.}$ and experimentally measured $F_{exp.}$ axial force of the brace for each axial displacement δ_i (total of N points) of the testing loading protocol,

$$H(\varepsilon_o, m) = \sqrt{\sum_{i=1}^{N} \left[F_{\exp.}(\delta_i) - F_{simul.}(\delta_i) \right]^2} \tag{2.3}$$

The objective function is non-differentiable; therefore the optimization problem lacks smoothness. However, the advantage of MADS is that it does not use information about the gradient of the objective function to search for an optimal point compared to more traditional optimization algorithms. Figure 2.4 illustrates examples of successful calibrations of the hysteretic response of steel braces that were tested cyclically through fracture under different loading histories. The comparisons indicate a fairly good match between the analytical and experimental results.

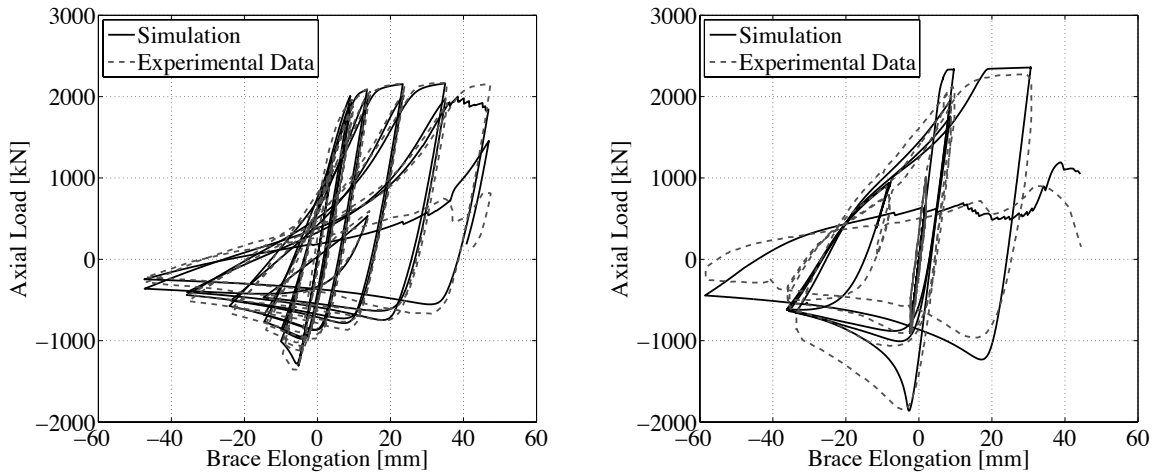

Figure 2.4 Calibration examples of the hysteretic behavior of steel braces (Data from Richard 2009 and Uriz and Mahin 2008)

2.3.3. Summary of Preliminary Findings

This section summarizes preliminary findings from the calibration study that was conducted for HSS braces. Emphasis is placed on the parameters ε_o and m that control fracture initiation of steel braces due to low cycle fatigue. The coefficient m in Eqn. 2.3 is typically determined by constant amplitude uniaxial tests (e.g., Ballio and Castiglioni 1995, Uriz and Mahin 2008). Since this information was not available for any of the collected tests, both ε_o and m values were evaluated as part of the calibration study discussed in Section 2.3.2. It was found that the coefficient m is constant regardless the shape of the steel brace that was calibrated. Figure 2.5 shows the effect of KL/r and b/t ratios of HSS steel braces on the coefficient m. Based on a t-test, it was found that none of the two parameters (KL/r, b/t) are statistically significant on m. Therefore m can be treated as a constant and equal to -0.3.

Figures 2.5c and 2.5d show the effect of *KL/r* and *b/t* ratios on the parameter ε_o. In this figure, the straight line does not represent a statistical curve. it just demonstrates the trends of ε_o with respect to the two geometric parameters. From Figure 2.5c, a slender brace (large *KL/r*) is more susceptible to fracture compared to a compact one, since ε_o becomes smaller in this case. From Fig. 2.5d, the parameter ε_o is somewhat dependent on the *b/t* ratio of an HSS brace. A brace with smaller *b/t* ratio will typically fracture later compared to a similar slenderness brace but larger *b/t* ratio under a similar loading protocol. This agrees with earlier quantitative findings by Tremblay (2002) on cold form HSS braces based on the effect of *KL/r* and *b/t* ratios on the total ductility reached at fracture. However, the effect of *b/t* ratio is typically more pronounced for braces with small *KL/r* ratios. Therefore, the correlations between *KL/r*, *b/t* and material properties of the steel braces should be taken into account to draw conclusions regarding the parameter ε_o. This investigation is underway.

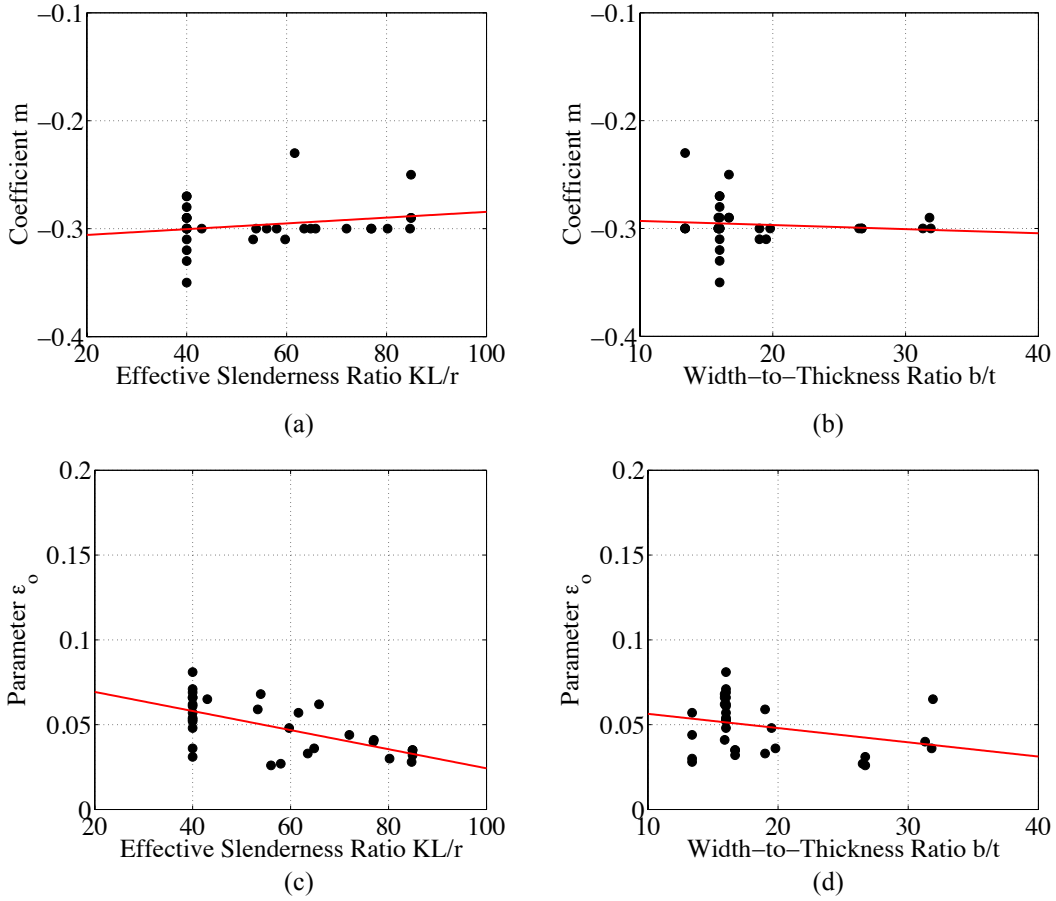

Figure 2.5 Effect of effective slenderness (*KL/r*) and depth-to-thickness ratios (*b/t*) on the parameters *m* and ε_o for HSS steel braces

3. CASE STUDY

The utilization of the steel brace database for modeling of post-buckling behavior and fracture of steel braces due to low-cycle fatigue is demonstrated through a case study of a SCBF, which was tested under static cyclic loading at the University of California at Berkeley by Uriz and Mahin (2008). The test specimen consists of a 2-story, one-bay chevron (inverted-V) configuration and was designed in accordance with AISC (1997). The steel braces were HSS152x152x9.5 (HSS6”x6”x3/8”) sections conforming to the specification for ASTM A500 grade B. The gusset plate connections were determined using the uniform force method (AISC 1993) and they allowed for a fold line equal to twice the thickness of the gusset plate, which was 22mm (7/8”). The steel braces were reinforced with steel plates in the connection region in order to prevent premature fractures at the reduced net area.

The geometry of the test specimen is shown in Fig. 3.1a. A 6700kN (1500kips) actuator was attached to the top floor beam of the test specimen to apply the AISC/SEAOC loading protocol, which was developed for testing of buckling-restraint braced frames. More details about the specimen, instrumentation and test results can be found in Uriz and Mahin (2008).

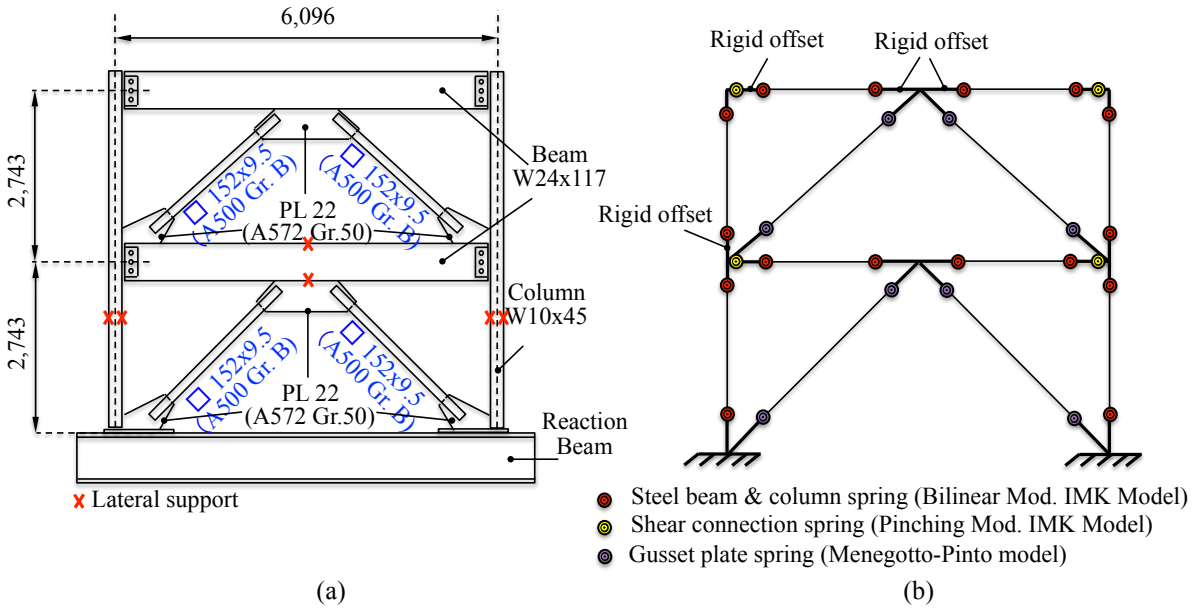

Figure 3.1 2-story SCBF; (a) geometry and material properties, (b) 2-D numerical model (units in mm)

A 2-dimensional (2-D) numerical model is built in OpenSees in order to simulate the performance of the SCBF. The steel columns are modeled with elastic elements and concentrated plasticity springs at their ends. These springs utilize the bilinear version of the modified Ibarra-Medina-Krawinkler (IMK) deterioration model (Ibarra et al. 2005, Lignos and Krawinkler 2011). This allows considering the cyclic deterioration in strength and stiffness of these columns. The parameters of these springs are determined based on multivariate regression equations developed by Lignos and Krawinkler (2011). The shear connections at the column faces are modelled with the pinching version of the modified IMK model. The properties of those springs were calibrated based on experimental data from Liu and Astaneh (2000). These tests do not consider the effect of gusset plates on the cyclic behavior of the shear connections; thus, a more realistic connection model should be utilized as discussed by Stoakes and Fahnestock (2011). The steel braces are modeled with the approach discussed in Section 2.3.1. The parameters that are used to model fracture due to low-cycle fatigue are determined based on the discussion in Section 2.3.3 given the *KL/r* and *b/t* ratios of the HSS braces of the test specimen. Rigid offsets are used (see Fig. 3.1b) to consider the effect of gusset plates on the beam-to-column connection regions. The flexibility and strength of the gusset plates is modeled with concentrated plasticity springs that are placed between the physical ends of the braces and the rigid offsets that represent the remainder of the gusset plates. These springs utilize the Menegotto-Pinto (1973) model. The flexural stiffness and strength of these springs is based on the Whitmore width and the relationships that were recently proposed by Hsiao et al. (2012).

Figure 3.2a shows the experimental base shear versus first story drift ratio (SDR) of the 2-story SCBF. In the same figure we have superimposed the simulated response based on the 2-D model shown in Fig. 3.1b. It is demontrated that the global response of the SCBF is represented reasonably well with this model including the cyclic deterioration in strength due to brace fracture. After brace fracture, a first story collapse mechanism is developed in the 2-story SCBF that includes plastic hinges at the top and bottom of the first story columns. This mechanism is also captured by the 2-D model including cyclic deterioration in strength of the same columns. Brace fracture is accurately traced by the 2-D model for both the north and south braces of the 2-story SCBF. A comparison of the simulated versus experimental axial force-brace elongation for the south brace is shown in Fig. 3.2b. The observed

differences between experimental and analytical results are attributed in part to the fact that during the tests, the brace force-elongation relationships were obtained with the virtual work equation and statics by utilizing elastic portions of the beam and columns and effectively ignoring the in-plane flexural resistance of the braces. The same models have been successfully validated with recent shake table tests of SCBFs conducted at the E-Defense facility in Japan (Okazaki et al. 2012).

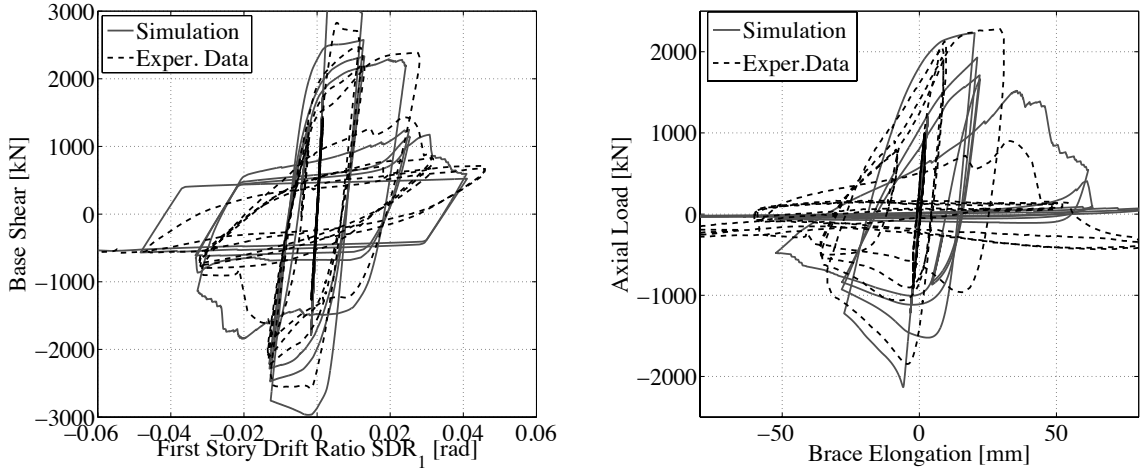

(a) Base shear first story drift ratio (b) South brace

Figure 3.2 Comparison of simulated and experimental data; (a) base shear first story drift ratio; (b) axial load-displacement of the south brace (data from Uriz and Mahin 2008)

4. SUMMARY AND CONCLUSIONS

This paper discusses the development of a steel brace database for modeling of the post-buckling behavior and fracture of steel braces as part of steel braced frames. The database includes 295 tests from 20 different experimental programs that have been conducted worldwide including the digitized histories of the axial force-displacement hysteretic response of steel braces with various shapes. The database serves for computing statistical information of the measured yield and ultimate stresses of various steel grades that are commonly used in design practice. Drift-based fragility curves are also developed for three major steel brace damage states. These damage states are associated with (1) flexural buckling, (2) local buckling and (3) strength loss due to low cyclic fatigue. This is particularly important for rapid estimation of earthquake damage based on peak story drift ratios of braced frames. A state-of-the art numerical model that is able to trace the hysteretic behavior of steel braces through fracture is extensively calibrated with the axial load-displacement hysteretic diagrams provided by the steel brace database. Based on the calibration effort, information is provided regarding the missing aspect of comprehensive numerical modelling of the post-buckling behavior and fracture due to low cycle fatigue of steel braces. This information is utilized through a case study of a 2-story SCBF. The proposed numerical model is able to predict fracture of both steel braces and the story collapse mechanism of the 2-story SCBF.

AKCNOWLEDGEMENT

The authors would like to sincerely thank Dr. Patxi Uriz and Professor Steve Mahin at the University of California, Berkeley, for kindly sharing the digitized data of the experiments they have conducted on steel braces during the past 8 years.

REFERENCES

Abramson, M.A., Audet, C., Chrissis, J.W. and Walston, J.G. (2009). Mesh adaptive direct search algorithms for mixed variable optimization. *Journal of Mathematics and Statistics*, **3:1**, 35-47.

AISC (1993). Load and resistance factor design LRFD. American Institute of Steel Construction, AISC, Chicago, Illinois.

AISC (1997). Seismic provisions for structural steel buildings. American Institute of Steel Construction, AISC, Chicago, Illinois.

AISC (2010). Specification for structural steel buildings. American Institute of Steel Construction, AISC-360-10, Chicago, Illinois.

Ballio, G. and Castiglioni, C.A. (1995). A unified approach for the design of steel structrues under low and/or high cyclic fatigue. *Journal of Constructional Steel Research*, **34**,75-101.

CISC (2010). Handbook of steel construction. *Canadian Institute of Steel Construction*, 10th Edition.

Fell, B. V. Kanvinde, A.M., Deierlein, G.G. and Myers, A.T. (2009). Experimental investigation of inelastic cyclic buckling and fracture of steel braces. *Journal of Structural Engineering*, ASCE **135:1**,19-32.

Hsiao, P.C., Lehman, D.E. and Roeder, C.W. (2012). Improved analytical model for special concentrically braced frames. *Journal of Constructional Steel Research*, **73**, 80-94.

Huang, Y. and Mahin, S.A. (2010). Simulating the inelastic seismic behavior of steel braced frames including the effects of low-cycle fatigue. *Report PEER 2010/104*, Pacific Earthquake Engineering Research Center, University of California at Berkeley, Berkeley, CA.

Ibarra, F. L., Medina, R.A and Krawinkler, H. (2005). Hysteretic models that incorporate strength and stiffness deterioration. *Earthquake Engineering and Structural Dynamics*, **34:12**, 1489-1511.

Ikeda, K., Mahin, S.A. and Dermitzakis, S.N. (1984). Phenomenological modeling of steel braces under cyclic loading. *Report No. UCB/EERC-84/09*, University of California, Berkeley.

Jin, J. and El-Tawil, S. (2003). Inelastic cyclic model for steel braces. *Journal of Structural Engineering*, ASCE **129:5**,548-557.

Krishnan, S. (2010). Modified elastofiber element for steel slender column and brace modeling. *Journal of Structural Engineering*, ASCE **136:11**,1350-1366.

Lee, K. and Bruneau, M. (2005). Energy dissipation of compression members in concentrically braced frames: review of experimental data. *Journal of Structural Engineering*, ASCE **131:4**, 552-559.

Lignos, D.G. (2008). Sidesway collapse of deteriorating structural systems under earthquakes. *PhD Dissertation*, Department of Civil and Environmental Engineeering, Stanford University, Stanford, CA.

Lignos, D.G. and Krawinkler, H. (2011). Deterioration modeling of steel components in support of collapse prediction of steel moment frames under earthquake loading. *Journal of Structural Engineering*, ASCE **137:11**,1291-1302.

Liu, J. and Astaneh, A.A. (2000). Cyclic testing of simple connections including effects of slab. *Journal of Structural Engineering*, ASCE, **126:1**, 32-39.

Manson, S.S. (1965). Fatigue, a complex subject: some simple approximations. *Journal of Experimental Mechanics*, **5**, 193-226.

Menegotto, M. and Pinto, P.E. (1973). Method of analysis for cyclically loaded reinforced concrete plane frames including changes in geometry and non-elastic behavior of elements under combined normal force and nending. *International Association of Bridge and Structural Engineering (IABSE),* Libson, Portugal, **Vol. 13**, 15-22.

McKenna, F. (1997). Object oriented finite element programming frameworks for analysis, algorithms and parallel processing. *PhD Dissertation*, University of California at Berkeley, Berkeley, CA.

Okazaki, T., Lignos, D.G., Hikino, T. and Kajiwara, K. (2012). Dynamic response of a chevron concentrically braced frame. *Journal of Structural Engineering*, ASCE (under review).

S16-09 (2009). Design of steel structures. *Canadian Standards Association*, Mississauga, Ontario, Canada.

Richard, J. (2009). Etude du comportement sismique de batiments industriels avec systemes de contreventement en acier de failble ductilite. *PhD Dissertation*, Department of Civil and Geotechnical and Mining Engineering, Ecole Polytechnique, Montreal, Canada (in French).

Spacone, E., Filippou, F.C. and Taucer, F.F. (1996). Fiber beam-column model for nonlinear analysis of RC frames. I: formulation. *Earthquake Engineering and Structural Dynamics* **25:7**, 711-725.

Stoakes, C.D. and Fahnestock, L.A. (2011). Cyclic flexural analysis and behavior of beam-column connections with gusset plates. *Journal of Constructional Steel Research*, **72**, 227-239.

Tremblay, R. (2002). Inelastic seismic response of steel bracing members. *Journal of Constructional Steel Research*, **58**, 665-701.

Uriz, P. and Mahin, S.A. (2008). Towards earthquake-resistant design of concentrically braced steel-frame structures. *Report PEER 2008/08*, Pacific Earthquake Engineering Research Center, University of California at Berkeley, Berkeley, CA.

Venables, W.N. and Ripley, B.D. (2002). Modern applied statistics with S, **4th Ed.**, Springer, New York.

Victorsson, V. K. (2011). The reliability of capacity-designed components in seismic resistant systems. *PhD Dissertation*, Department of Civil and Environmental Engineering, Stanford University, Stanford, CA.